# Observation and modeling of the Earth-ionosphere cavity electromagnetic transverse resonance and variation of the D-region electron density near sunset

Fernando Simões, Jean-Jacques Berthelier, Michel Godefroy, Sahed Yahi

# Observation and modeling of the Earth-ionosphere cavity electromagnetic transverse resonance and variation of the D-region electron density near sunset

F. Simões,[1] J.-J. Berthelier,[1] M. Godefroy,[1] and S. Yahi[1]

[1] In the frame of the African Monsoon Multidisciplinary Analyses campaign, measurements of very low frequency electric fields were performed onboard a stratospheric balloon launched on 7 August 2006 from Niamey, Niger. During flight, numerous sferics were observed associated to lightning from active convective cells a few hundred kilometers from the balloon. Lightning data analysis shows the transverse mode mean frequency of the Earth-ionosphere cavity decreasing from ∼2.4 to 2 kHz over a period of 1 h about sunset. The observed change of the transverse resonance near dusk can be fairly reproduced by an electromagnetic wave propagation model, which takes into account the D-region electron density variation predicted by the International Reference Ionosphere model. **Citation:** Simões, F., J.-J. Berthelier, M. Godefroy, and S. Yahi (2009), Observation and modeling of the Earth-ionosphere cavity electromagnetic transverse resonance and variation of the D-region electron density near sunset, *Geophys. Res. Lett.*, *36*, L14816, doi:10.1029/2009GL039286.

## 1. Introduction

[2] The propagation of Extremely Low Frequency (ELF) and Very Low Frequency (VLF) electromagnetic waves originating from lightning has been extensively studied to investigate the characteristics of the Earth-ionosphere cavity, in particular through the ELF longitudinal modes known as Schumann resonance [*Schumann*, 1952]. In addition to these modes that are a large scale phenomenon characteristic of the global propagation of electromagnetic waves around the Earth, transverse resonance modes can be excited in the VLF domain [*Nickolaenko and Hayakawa*, 2002; *Helliwell*, 2006]. When the shells that form the cavity are perfect electric conductors, the transverse mode requires null electric field at the boundaries. A resonance develops whenever the separation between the shells, generally the height of the ionosphere, $h$, is an integer number, $n$, of half-wavelengths,

$$\omega_n = n \frac{c\pi}{h} \frac{1}{\sqrt{1 - \sin^2 \theta}}, \qquad (1)$$

where $\omega_n$ is the angular frequency of mode $n$, $\theta$ the angle between the wave vector and the vertical direction, and $c$ the velocity of light in the medium [*Wait*, 1962].

[3] Considering an ionospheric effective height of 75 km, one obtains about 2 kHz for the first transverse mode though frequencies between 1.5 and 2.5 kHz have been reported [e.g., *Cummer et al.*, 1998; *Nickolaenko and Hayakawa*, 2002]. Whereas the longitudinal mode can be used to study the global characteristics of the lower ionosphere, the transverse mode responds to local variations only. Hence, monitoring of the transverse mode contributes to investigating local ionospheric variability and heterogeneity, for example the day-night transition. Impulsive electromagnetic signals, namely those originating from lightning discharges, have indeed contributed to the investigation of wave propagation in the Earth-ionosphere waveguide and to remote sensing of the ionospheric D-region [*Hayakawa et al.*, 1994; *Shvets and Hayakawa*, 1998; *Peter and Inan*, 2007; *Jacobson et al.*, 2008, and references therein].

[4] In this paper we report VLF electric field measurements made onboard a stratospheric balloon during the African Monsoon Multidisciplinary Analyses (AMMA) SCOUT campaign. The balloon flight lasted about 3 h, encompassing the time of sunset, thus contributing to assessing the variation of the propagation conditions due to the D-region electron density changing. After a brief description of the experiment and atmospheric conditions of the flight, we provide the results of an analysis of several hundred impulsive electromagnetic events for which the transverse resonance mode was clearly identified. These observations are in fair agreement with a wave propagation model that considers an electron density distribution near dusk derived from the International Reference Ionosphere (IRI) model.

## 2. Experiment Description

[5] The HV-AIRS (High Voltage - Atmospheric Impact of Radiations and Sprites) electric field experiment was part of a multiple instrument flight chain that included other sensors devoted to observations of aerosols and atmospheric composition. It measures the atmospheric electric field from DC to ∼4 kHz employing the double probe technique [*Mozer and Serlin*, 1969], which has been widely used onboard balloons to measure stratospheric electric fields. The effective length of the antenna is about 40 cm. The DC and AC components of the electric field are measured in two channels: (i) large amplitude signals in the so-called "DC channel", which provides the DC electric field measurements and covers the whole frequency range from 0 to ∼4 kHz; (ii) small amplitude AC signals in the so-called "AC channel" between 4 Hz and 4 kHz. The electronics is designed to measure electrode potentials from −110 V to +110 V, corresponding to a range of ±300 Vm⁻¹ for the

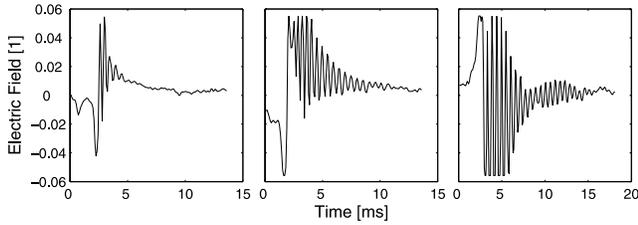[1]LATMOS, IPSL, CNRS, Saint-Maur, France.

**Figure 1.** Typical (left) day and (middle) night sferics recorded by HV-AIRS onboard the stratospheric balloon at altitude of about 20 km. (right) Distinctive tweek recorded during nighttime at 19 km. From left, the frequency and wave damping are 2.25, 2.04, 1.78 kHz, and 3, 0.75, 0.65 dB Mm$^{-1}$. Typical tweek wave damping found in literature is 0.4 dB Mm$^{-1}$.

electric field in the DC channel. The AC channel has a noise level of 30 $\mu$Vm$^{-1}$ Hz$^{-1/2}$ and 3 gains that allow measuring AC electric fields up to ±2.5 Vm$^{-1}$. The HV-AIRS gondola also included simple optical detectors to identify lightning as far as ~300 km after sunset and a GPS receiver.

## 3. Flight Conditions

[6] The experiment took place on 7 August 2006 in Niamey, Niger, and the balloon was launched at T0 = 1645 UT. With an ascent velocity of ~5 ms$^{-1}$, the balloon reached the ceiling altitude of 23 km at 1802 UT, traveling (~200 km) almost exactly westward until the end of the flight. During the ceiling period, the balloon altitude decreased slowly down to about 20 km after 1845 UT; the last measurements were recorded at 19 km. The sunset at the balloon position occurred at 1843 UT (T$_B$, 118 min from T0); the sunset at the position of the strongest local convective system (~400 km east of the balloon final position) and in the D-region above occurred 93 (T$_S$) and 130 min (T$_D$) from T0, respectively.

[7] Upon ascent, the balloon crossed a series of clouds displaying no electrical activity and the downward pointing DC vertical electric field was rather typical of fair weather conditions with moderate amplitude of ~2.5 Vm$^{-1}$ at ceiling altitude. Images from the AMMA campaign meteorological radar (see the AMMA data center at http://aoc.amma-international.org) showed active, though variable, convective systems about ~100 km east and south of Niamey during the flight. At about 200 km west of Niamey, a weaker though persistent convective system was active during the entire flight. Numerous lightning and strong electric field signals were observed.

## 4. Results

[8] The AC electric field channel recorded a few thousand impulsive events, namely about 700 sferics and a few tweeks showing detectable transverse resonances. An example is displayed in Figure 1 with three typical waveforms recorded before and after sunset. Three approaches were tested to compute the waveform mean period, namely the method of least squares applied to damped sinusoidal functions, Fourier analysis, and crest-crest period counting. Because of waveform variability, occasional receiver saturation, and DC electric field significant contribution, the

crest-crest period counting is the most effective approach to extract the mean frequency from each signal. The average time window is 20 ms. As expected, the damping of electromagnetic waves is more pronounced during daytime due to losses in the more conductive lower D-region and often prevents frequency evaluation. On the contrary, the conductivity profile of the nightside is steeper and provides better propagation conditions with the resonant wave showing up to 20 periods (Figure 1).

[9] Figure 2 shows the frequencies extracted from sferics and tweeks; the squares correspond to the mean frequency best fitting each waveform (Figure 2, left). The number of data points is about 70 and 620 before and after the kink (~1800 UT). The error associated to frequency estimation using the crest-crest period counting method is about 90 and 40 Hz before and after the kink. The solid line and the error bars correspond to the mean and standard deviation calculated over 30 min periods. The circles are values computed with our numerical model employing IRI electron density distributions.

[10] Since sferics distribution during the balloon flight shows some regular patterns it is useful to verify which frequencies occur more often; a histogram of the resonance frequencies is shown in Figure 2 (right). As expected from results above, the histogram shows that not only the resonant frequencies are centered at ~2 kHz but lines at 1.85, 2.02, and 2.22 kHz seem statistically significant.

## 5. Modeling

[11] To interpret the balloon data, we have developed a wave propagation finite element model (WP-FEM) that benefits from algorithms previously used to study wave propagation on Earth and other planetary environments [*Simões et al.*, 2008a, 2008b]. We consider that lightning discharges occur at 10 km, which is appropriate to simulating cloud-to-ground and ground-to-cloud (vertical) and inter-cloud (horizontal) lightning in tropical convective systems. The source, i.e., the lightning discharge, is fairly well represented by a Hertz dipole and the algorithm solves Maxwell equations in a 3D configuration of the Earth-ionosphere waveguide. The model can be run either in the harmonic propagation mode, where the computations are performed for a number of discrete frequencies, or in the transient mode, where the dipole temporal variation reproduces the lightning current [*Simões et al.*, 2007]. The stationary mode computes the electric field spectrum of the waveguide in the range 0–10 kHz. A representative current profile [see *Rakov and Uman*, 2003, Table 4.12 and Figure 4.55] is used in the transient mode. The atmospheric conductivity profile below 50 km was defined according to the works of *Volland* [1982] and *Holzworth* [1995]. Above 50 km, we use the IRI, International Geomagnetic Reference Field, and International Standard Atmosphere models to derive the electron density, magnetic field, and collision frequency that are required to calculate the conductivity tensor [*Simões*, 2007].

[12] Figure 3 presents waveforms of the electric field at the balloon ceiling altitude computed with the transient method. The discharge starts at $t$ = 1 ms and the electric field, **E**, is computed in several locations, i.e., for various angular separations between the radiating source and the
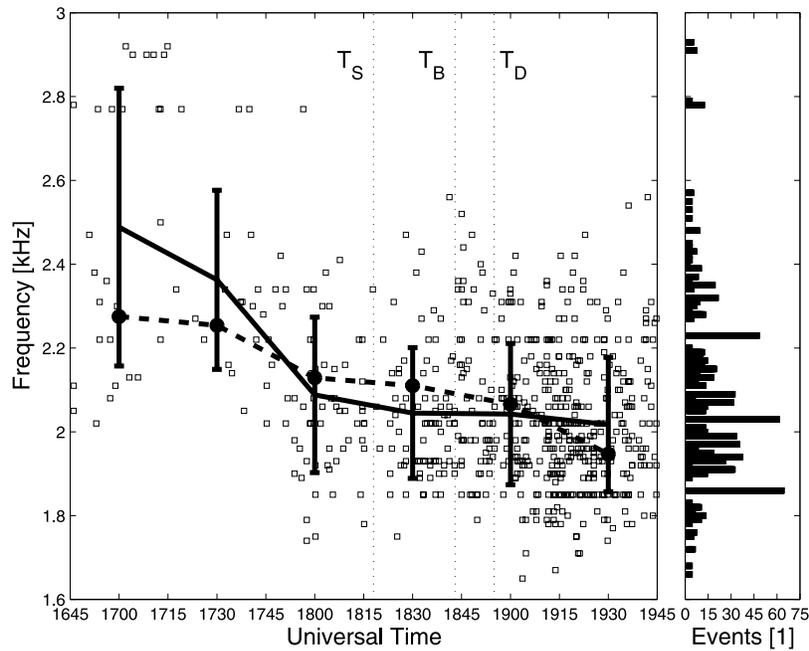
**Figure 2.** Frequencies extracted from sferics and tweeks. (left) Squares correspond to the frequency of individual impulsive events; the solid line and error bars represent the mean value and standard deviation calculated over periods of 30 min. The circles/dashed line are numerical results using IRI electron density distributions. The labels $T_S$, $T_B$, and $T_D$ represent the sunset time at the strongest convective cell, balloon position, and the D-region above the convective cell, respectively. (right) Histogram of impulsive events as function of the mean frequency measured during the flight.

balloon. The waveform frequency is ~2 kHz and the propagation delay increases with angular separation. Whereas at large distances ($r$) the electromagnetic component ($E \propto 1/r$) is dominant, the electrostatic contribution ($E \propto 1/r^3$) is more significant close to the source. Figure 3 shows the decrease of the DC contribution with angular separation. Although an accurate characterization of lightning strokes by their intensity, duration, distance, and direction requires triangulation and receiver synchronization, it is possible to estimate the source distance from waveform morphology, i.e., shape, attenuation, and DC component contribution. Comparison between the balloon data and model waveforms suggests that about 75% of the recorded lightning occurred not farther than 350 km, i.e., ~3° of angular separation.

[13] Employing a simple analytical approximation based on the Appleton-Hartree equation that describes the refractive index in cold magnetized plasma, it is possible to estimate the altitude at which the VLF waves are reflected. A first estimation can be made considering an isotropic medium and the condition of total reflection - equalizing Joule and displacement currents [e.g., *Shvets and Hayakawa*, 1998]. Calculation of the electron density, $N_e$, at the reflection altitude yields

$$N_e = \frac{\omega m \varepsilon_o \nu_{eff}}{e^2}, \qquad (2)$$

where $\nu_{eff}$ is the effective collision frequency of electrons with neutrals, $e$ and $m$ are the electron charge and mass, and $\varepsilon_o$ is the permittivity of vacuum. Equations (1) and (2) are used to obtain rough estimates of the ionospheric reflection height and corresponding electron density recorded for each

impulsive event. However, accurate estimations require electron density and magnetic field 3D parameterization (see *Simões* [2007] for details about the numerical model).

## 6. Discussion and Conclusion

[14] The sharper gradient of the electron density profile in the D-region during nighttime provides better propagation conditions and consequently the observed damping of the
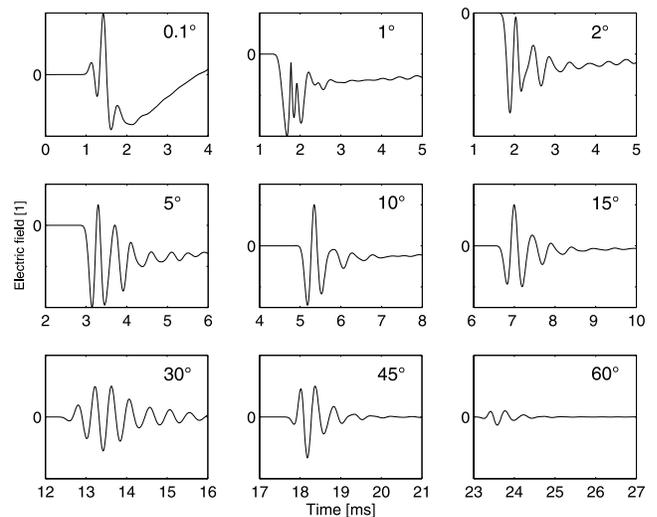


**Figure 3.** Waveforms of a lightning discharge calculated with the transient mode algorithm at several angular separations from the source. The electric field is in arbitrary units and the time axis shifting testifies retarded propagation at different angles.

**Table 1.** Ionospheric Reflection Altitude Estimations Inferred From Tweeks[a]

| Measurement Location | Altitude-Day [km] | Altitude-Night [km] | Reference |
|---|---|---|---|
| 18°S, 178°E | (70−75) | 85−90 | *Kumar et al.* [2008] |
| 44°N, 142°E; 31°N, 131°E | - | 79−90 | *Ohya et al.* [2006] |
| 37°N, 122°W | - | 81−85 | *Cummer et al.* [1998] |
| 18°S, 7°E; 21°S, 66°E | - | 81−88 | *Shvets and Hayakawa* [1998] |
| 21°N, 110°E; 25°N, 110°E; 30°N, 115°E | - | 83−95 | *Hayakawa et al.* [1994] |

[a]The range between brackets corresponds to model estimations rather than measurements.

transverse resonance is weaker after sunset, showing up to ∼20 periods in contrast to ∼5 periods before dusk. Together with a higher occurrence of thunderstorms in the late afternoon, this fact certainly explains why most works published so far deal with nighttime events (Table 1). However, the present dataset allows us to extent such analysis to daytime as well.

[15] A detailed quantitative comparison between our model and other observations is difficult due to lightning discharges and ionospheric conditions variability. However, the frequency spectra computed in the harmonic propagation mode (not shown here) reproduce the main features of the measured spectra shown by *Nickolaenko and Hayakawa* [2002, Figure 6.46], and the transient mode simulations replicate quite well our measurements (Figures 1 and 3) as well as waveforms recorded by other teams [*Rakov and Uman*, 2003, Figure 13.8].

[16] The electron density corresponding to the wave reflection altitude derived from equation (2) is about 10 cm$^{-3}$, close to the electron density of ∼25 cm$^{-3}$ estimated by *Shvets and Hayakawa* [1998], though these analytical approximations are not accurate enough. Table 2 shows the mean frequency of sferics for day and nighttime and the reflection altitude computed under several approximations. Comparison between the numerical model and balloon data shows frequency falling within the error range (Figure 2). The discrepancy among nighttime results shown in Tables 1 and 2 is expected because our data are recorded close to sunset, when the ionosphere has not yet reached an ionization minimum.

[17] We have compared the electron density at the reflection altitude with the IRI model [*Bilitza and Reinisch*, 2008]. Figure 4 shows the reflection altitude vs. time calculated with the numerical model and equation (2); in the later, wee seek for the altitude in the plot that corresponds to the computed electron density. A few curves of constant electron density are shown for comparison purposes. Comparison between Table 2 and Figure 4 shows that the Appleton-Hartree approximation does not provide accurate electron density estimates of the reflection altitude. Corroborating our model, *Cummer et al.* [1998] also found

electron densities tenfold higher than that computed with equation (2). Analysis of Figures 2 and 4 suggests: i) frequency measurements and numerical results concur; ii) balloon data and IRI electron densities are reasonably consistent; iii) the day-night frequency/reflection altitude variation is smoother than that of electron density; iv) unlike what might be expected, the maximum variation of reflection altitude and electron density does not coincide (offset >30 min). Since no obvious explanation is found for the time offset, a better characterization of sferics frequency and, more importantly, of lightning location needed to assess such discrepancy will be undertaken in the near future. Other possible explanations include IRI model inaccuracy near sunset or specific ionospheric perturbations in the day of the flight.

[18] As expected, the histogram of Figure 2 shows a broad peak at about 2 kHz; additionally, 3 prominent lines appear at 1.85, 2.02, and 2.22 kHz. If we consider that resonance frequencies spreading stems from the natural variability of the ionosphere and of propagation conditions over a wide thunderstorm area, the uneven spectrum may be explained by the presence of localized active convective cells with increased lightning rate. Additional information
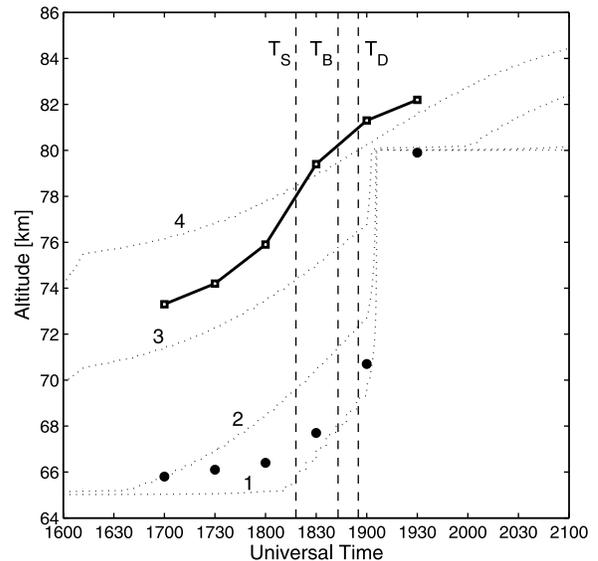


**Figure 4.** Average reflection altitude as function of time derived from the numerical model (squares) and the Appleton-Hartree approximation (circles). The dotted lines 1−4 correspond to electron isodensity of 3, 25, 150, and 300 cm$^{-3}$, respectively, derived from the IRI model at 13°N, 2°E. The sharp transition of the electron density at ∼19 h corresponds to the local sunset at the D-layer. For details about the vertical dashed lines see Figure 2.

**Table 2.** Transverse Mode Average Frequency and Reflection Altitude[a]

| Universal Time | 1200 | 1700 | 1930 | 0000 |
|---|---|---|---|---|
| Measured Frequency [kHz] | - | 2.42 ± 0.27 | 2.05 ± 0.16 | - |
| WP-FEM − Frequency [kHz] | 2.29 | 2.27 | 1.94 | 1.81 |
| WP-FEM − Altitude [km] | 72 | 73 | 82 | 88 |
| Equation (2) − Altitude [km] | 65 | 66 | 80 | 83 |
| Equation (1) − Altitude [km] | - | 63 | 73 | - |

[a]In the case of the numerical model, the reflection altitude is chosen where the electric field of the transverse mode is reduced to 1%.

of lightning characteristics, namely polarization, should permit refined analyses of the AMMA balloon data.

[19] We have shown that lightning is a valuable tool to study the day-night transition of the ionospheric D-region. Therefore, and since the D-region is rather difficult to explore both with remote sensing and in situ techniques, systematic high resolution measurements of sferics and respective sources made with lightning location networks provide a suitable tool to monitoring the electron density profiles. Careful monitoring of the ionospheric day-night variation also provides insights on the D-region ionization chemical processes.

# References

Bilitza, D., and B. Reinisch (2008), International Reference Ionosphere 2007: Improvements and new parameters, *Adv. Space Res.*, *42*, 599–609, doi:10.1016/j.asr.2007.07.048.

Cummer, S. A., U. S. Inan, and T. F. Bell (1998), Ionospheric D region remote sensing using VLF radio atmospherics, *Radio Sci.*, *33*, 1781–1792, doi:10.1029/98RS02381.

Hayakawa, M., K. Ohta, and K. Baba (1994), Wave characteristics of tweek atmospherics deduced from the direction-finding measurement and theoretical interpretation, *J. Geophys. Res.*, *99*, 10,733–10,743, doi:10.1029/93JD02555.

Helliwell, R. (2006), *Whistlers and Related Ionospheric Phenomena*, 2nd ed., Dover, Mineola, N. Y.

Holzworth, R. H. (1995), Quasistatic electromagnetic phenomena in the atmosphere and ionosphere, in *Handbook of Atmospheric Electrodynamics*, vol. 1, edited by H. Volland, pp. 235–266, CRC Press, Boca Raton, Fla.

Jacobson, A. R., R. Holzworth, and X.-M. Shao (2008), Low-frequency ionospheric sounding with Narrow Bipolar Event lightning radio emissions: Energy-reflectivity spectrum, *Ann. Geophys.*, *26*, 1793–1803.

Kumar, S., A. Kishore, and V. Ramachandran (2008), Higher harmonic tweek sferics observed at low latitude: Estimation of VLF reflection heights and tweek propagation distance, *Ann. Geophys.*, *26*, 1451–1459.

Mozer, F. S., and R. Serlin (1969), Magnetospheric electric field measurements with balloons, *J. Geophys. Res.*, *74*, 4739–4754, doi:10.1029/JA074i019p04739.

Nickolaenko, A. P., and M. Hayakawa (2002), *Resonances in the Earth-Ionosphere Cavity*, Kluwer Acad., Dordrecht, Netherlands.

Ohya, H., M. Nishino, Y. Murayama, K. Igarashi, and A. Saito (2006), Using tweek atmospherics to measure the response of the low-middle latitude D-region ionosphere to a magnetic storm, *J. Atmos. Sol. Terr. Phys.*, *68*, 697–709, doi:10.1016/j.jastp.2005.10.014.

Peter, W. B., and U. S. Inan (2007), A quantitative comparison of lightning-induced electron precipitation and VLF signal perturbations, *J. Geophys. Res.*, *112*, A12212, doi:10.1029/2006JA012165.

Rakov, V., and M. Uman (2003), *Lightning*, Cambridge Univ. Press, Cambridge, U. K.

Schumann, W. O. (1952), On the free oscillations of a conducting sphere which is surrounded by an air layer and an ionosphere shell (in German), *Z. Naturforsch. A*, *7*, 149–154.

Shvets, A. V., and M. Hayakawa (1998), Polarisation effects for tweek propagation, *J. Atmos. Sol. Terr. Phys.*, *60*, 461–469, doi:10.1016/S1364-6826(97)00131-4.

Simões, F. (2007), Theoretical and experimental studies of electromagnetic resonances in the ionospheric cavities of planets and satellites; instrument and mission perspectives, Ph.D. thesis, Université Pierre et Marie Curie, Paris 6, France.

Simões, F., et al. (2007), A new numerical model for the simulation of ELF wave propagation and the computation of eigenmodes in the atmosphere of Titan: Did Huygens observe any Schumann resonance?, *Planet. Space Sci.*, *55*, 1978–1989, doi:10.1016/j.pss.2007.04.016.

Simões, F., et al. (2008a), Electromagnetic wave propagation in the surface-ionosphere cavity of Venus, *J. Geophys. Res.*, *113*, E07007, doi:10.1029/2007JE003045.

Simões, F., et al. (2008b), The Schumann resonance: A tool for exploring the atmospheric environment and the subsurface of the planets and their satellites, *Icarus*, *194*, 30–41, doi:10.1016/j.icarus.2007.09.020.

Volland, H. (1982), Quasi-electrostatic fields within the atmosphere, in *Handbook of Atmospherics*, vol. 1, edited by H. Volland, pp. 65–106, CRC Press, Boca Raton, Fla.

Wait, J. (1962), *Electromagnetic Waves in Stratified Media*, Pergamon, Oxford, U. K.

———————

J.-J. Berthelier, M. Godefroy, F. Simões, and S. Yahi, LATMOS, IPSL, CNRS, 4 avenue de Neptune, F-94107 Saint-Maur CEDEX, France. (fernando.simoes@latmos.ipsl.fr)